

BMB Reports – Manuscript Submission

Manuscript Draft

DOI: [10.5483/BMBRep.2023-0004](https://doi.org/10.5483/BMBRep.2023-0004)

Manuscript Number: BMB-23-004

Title: The couple of netrin-1/ α -Synuclein regulates the survival of dopaminergic neurons via α -Synuclein disaggregation

Article Type: Article

Keywords: α -Synuclein; Netrin-1; Molecular interaction; Dopaminergic neuron; Parkinson's disease

Corresponding Author: Eun Hee Ahn

Authors: Eun Ji Kang¹, Seung Min Jang¹, Ye Ji Lee¹, Ye Ji Jeong¹, You Jin Kim¹, Seong Su Kang², Eun Hee Ahn^{1,*}

Institution: ¹Department of Physiology, Hallym University College of Medicine,
²Department of Pathology and Laboratory Medicine, Emory University College of Medicine,

The couple of netrin-1/ α -Synuclein regulates the survival of dopaminergic neurons via α -Synuclein disaggregation

Eun Ji Kang¹, Seung Min Jang¹, Ye Ji Lee¹, Ye Ji Jeong¹, You Jin Kim¹, Seong Su Kang², and Eun Hee Ahn^{1*}

¹Department of Physiology, College of Medicine, Hallym University, Hallymdaehak-gil 1, Chuncheon-si, Gangwon-Do 24252, South Korea

²Department of Pathology and Laboratory Medicine, Emory University School of Medicine, Atlanta, GA 30322, USA

Address for correspondence

Prof. Eun Hee Ahn

Telephone : +82-33-248-2583

Email : eunhee.ahn@hallym.ac.kr

Running title

Netrin-1/ α -Synuclein regulates α -Synucleinopathy

Abstract

The abnormal accumulation and aggregation of the misfolded α -Synuclein protein is the neuropathological hallmark of all α -Synucleinopathies, including Parkinson's disease. Netrins (netrin-1, netrin-3, and netrin-4) are secreted proteins, which are laminin-related and involved in axon guidance function and cell survival molecular pathway. Remarkably, only netrin-1 is highly expressed in healthy adult substantia nigra brain region and inversely correlates with the expression of α -Synuclein, which led us to investigate the impact of the molecular interaction between α -Synuclein and netrin-1 in dopaminergic neuron fate. Here we show that netrin-1 and α -Synuclein directly interact in pre-formed fibrils (PFFs) generation test, real time binding assay, and Co-Immunoprecipitation with neurotoxin treated cell lysates. Our findings suggest that netrin-1 deprivation triggers dopaminergic neuronal cell death signal pathway with α -Synuclein aggregation and hyperphosphorylates α -Synuclein S129. Taken together, netrin-1 can be

the promising therapeutic molecule in Parkinson's disease.

Keywords

α -Synuclein; Netrin-1; Molecule-molecule interaction; Dopaminergic neuron; Parkinson's disease;

Introduction

The netrin family (netrin-1, netrin-3 and netrin-4) are secreted proteins that administer the migration and control the axonal guidance as a multifunctional plasticity cue (1, 2). During development, it is well expressed in neuroepithelial cells of the spinal cord (3). Netrin-1, -3, and -4 proteins are involved the Laminin VI, Laminin V, and C345C domains, which is partially included in binding to the netrin receptors (UNC5) (4). Netrin-1, -3, and -4 share protein structural domains, but the brain regions for the protein expression are different with specific neuronal cell types (5, 6). Especially, Netrin-1 protein is expressed in ventral tegmental area (VTA), substantia nigra (SN), and striatum (Str), which is related to the dopaminergic neurons (7, 8). Dopaminergic neuron is known to be specifically vulnerable to neurodegeneration in Parkinson's disease (PD) (9, 10). The progressive degeneration of dopaminergic neurons of the substantia nigra pars compacta (SNpc) in PD leads to disabling motor symptoms decreasing the quality of common life of patients with PD (11). Numerous PD molecular studies have been reported that α -Synuclein aggregation and hyperphosphorylation trigger dopaminergic neuronal cell death and initiate the PD progression (12). Unfortunately, the etiology of the PD is still not clear and current medications are symptomatic and do not prevent the progression of the PD pathology. Therefore, we investigated the α -Synuclein's direct interaction with netrin-1 in the specific dopaminergic neuron. Consequently, netrin-1 robustly reduces α -Synuclein aggregation form and hyperphosphorylation, inhibiting dopaminergic neuronal loss and motor dysfunctions. Given that netrin-1 expression in mature dopaminergic neurons and its well-known role in cell survival as a dependent secreted protein, we investigated the impact of netrin-1 in the fate of dopaminergic neurons.

Results

The netrin-1 is significantly reduced in the substantia nigra of PD patients

α -Synuclein overexpressions are reported in aging human substantia nigra brain region (13, 14) leading to Lewy body formation with highly phosphorylated α -Synuclein S129 (15). To address importance of the netrin-1 in dopaminergic neurons, we confirmed the expression of netrin-1 in the substantia nigra (SN), which is related to the PD progression. We compared mRNA expression of netrin-1 in the SN of healthy controls or age-matched PD patients using a Gene expression omnibus (GEO) dataset GDS2821. We observed that the expression of human netrin-1 was significantly reduced in the SN region of PD patients compared to age-matched healthy control group (Fig. 1A, left). However, there are no differences in mRNA expression of PD between netrin-3 (Fig. 1A, middle) and netrin-4 (Fig. 1A, right). Next, to identify direct α -Synuclein's interaction with the netrin family, we applied the α -Synuclein keyword to the reprogramming software system (GeneMANIA). According to the programming software analysis, netrin-1 interacts directly with α -Synuclein (Fig. 1B). We observed the netrin-3 and netrin-4 were not involved in the α -Synuclein molecular interactions (Fig. 1C; Fig. 1D). Moreover, we looked at Allen Human Brain Atlas microarray database to determine the expression of netrin-1, -3, and -4 of PD and non-PD brain tissues in human (Fig. 1E) and mouse (Supplementary Fig. 1A-C). Interestingly, the mRNA expression of netrin-1 is the highest one among them in the SN. But, netrin-3 and netrin-4 were expressed much less than netrin-1 in the healthy control group (Supplementary Fig. 1D). We isolated the 20 candidates and classified the subjects of netrin-1, -3, and -4 proteins according to the dynamic expression during neuronal cell survival signaling activation via predicted protein interaction reprogramming (Supplementary Fig. 1 E). These results clearly presented the interactions of the netrin-1, -3 and -4 with α -Synuclein molecules.

Netrin-1 and SNCA directly interacts

We examined the binding affinity of netrins and α -Synuclein employing purified recombinant proteins via in vitro binding assay of SPR Biacore X100. Strikingly, real time binding assay demonstrated strong interaction between netrin-1 and α -Synuclein (Fig. 2A). However, there recombinant netrin-3 and netrin-4 proteins on α -Synuclein-immobilized CM5 chip did not show any interaction in SPR Biacore X100 analysis. Furthermore, we investigated the predictive interacting sites between netrin-1 and α -Synuclein proteins. We obtained a three-dimensional structure model of both proteins, including the predictive interaction sites by ClusPro 2.0. As a result, three types of structures (balanced, electrostatic-favored, and van der Waals force-favored) showed the polar contacts between netrin-1 and

124th – 135th amino acids in C-terminus of α -Synuclein. (Fig. 2B-D). Quantitative RT-PCR (qRT-PCR) demonstrated that the mRNA augmentation of α -Synuclein and MAO-B in SH-SY5Y cells by MPP⁺ was inversely coupled with netrin-1 mRNA (Supplementary Fig. 2A). And, to investigate whether recombinant netrin-1 regulates the phosphorylation of α -Synuclein at residue S129 in the progression of SH-SY5Y or rat cortical neuronal (DIV 10) cell death, we infected AAV2-SNCA during 48 h, then SH-SY5Y cells and DIV 10 primary neurons were treated with 200 ng of recombinant netrin-1 protein for 24 h. In vitro, this recombinant netrin-1 effectively inhibited the phosphorylated α -Synuclein S129 and improved cell viability (Supplementary Fig. 2B-D).

Netrin-1 deprivation initiates α -Synuclein aggregation in the primary dopaminergic neurons, inducing PD pathogenesis

We applied the 4th fibronectin domain of Deleted in Colorectal Cancer (DCC-4Fbn), which binds to netrin-1, in the primary dopaminergic neuronal cell to generate the netrin-1 deprived cellular model (8). Immunofluorescence (Fig. 3A-B) and TUNEL (Fig. 3C-D) analyses demonstrated that blocking netrin-1 via DCC-4Fbn in the primary dopaminergic neurons induced α -Synuclein phosphorylation and DNA fragmentation clearly. Consistent observations were made from primary dopaminergic neuronal cell lysates (Fig. 3E). In addition, overexpressed SNCA or deprived netrin-1 in dopaminergic neurons both increased the α -Synuclein S129 phosphorylation and reduced the netrin-1 expression as shown in the co-immunofluorescence staining (Supplementary Fig. 3A-B) (16). Western blotting revealed that MPP⁺ treatment dose-dependently reduced both netrin-1 and tyrosine hydroxylase (TH), and inversely elevated α -Synuclein and phosphorylation on S129 residue of α -Synuclein in the insoluble fraction cell lysates. In addition, monoamine oxidase B(MAO-B), which is the major enzyme for dopamine metabolism and activated in PD were escalated by MPP⁺ in a dose-dependent manner. For the netin-3 and netrin-4, we applied the 120 μ g of SH-SY5Y cell lysates due to the low expression in SH-SY5Y cell (Fig. 3F).

Netrin-1 involves neurorestorative effects in cellular model of PD

Now, we investigated whether, inversely, netrin-1 gain of function might protect or rescue the dopamine cells from cell death. We performed the qRT-PCR to confirm the α -Synuclein and netrin-1 mRNA levels with or without netrin-1 reintroduction (Supplementary Fig. 4A & C). Netrin-1 depletion was achieved by treating MPP⁺ neurotoxin or DCC-

4Fbn into the cell media. Next, we applied the netrin-1 protein dose-dependently via qRT-PCR and immunoblotting. Of interest, the reintroduced netrin-1 in dopaminergic cells induced the activation of the TH and netrin-1 expression with the PD-related marker proteins, MAO-B, cleaved casepase-3, α -Synuclein FL (Syn 204), and α -Synuclein S129 reductions (Supplementary Fig. 4B & D). In accordance with our previous result, we observed the DCF-DA (intracellular oxidative stress) signal reduction in netrin-1 treated with DCC-4Fbn group only (Supplementary Fig. 4E top) and obtained the similar observation in TUNEL assay (Supplementary Fig. 4E bottom). These results prove that netrin-1 is required for the maintenance and protection of dopaminergic neuron in adult.

Netrin-1 blocks α -Synuclein aggregation via direct interaction in the pure in-vitro analysis.

Thioflavin T (Th-T) α -Synuclein fibrillization kinetic assay showed that α -Synuclein formed the aggregated fibers in reaction day-dependent manner. The aggregation rate of α -Synuclein + netrin-1 (1:1 ratio) mixture was significantly lower than α -Synuclein only group (Fig. 4A and Fig. 4B). Stalks from each sample gave rise to anisotropic X-ray diffraction patterns displaying the typical features of a cross- β substructure, with axial inter-strand reflections at ~ 4.5 Å for α -Synuclein. α -Synuclein only group and α -Synuclein + netrin-1 mixture group showed the different x-ray count numbers via XRD crystallographic structure analysis. Meaningfully, α -Synuclein + netrin-1 mixture group reduced total PFFs intensity number 5795.588 to 1990.044 (Fig. 4C and Fig. 4D). Moreover, transmission electron microscopy (TEM) showed that PFFs of α -Synuclein + netrin-1 were much less than α -Synuclein only group (Fig. 4E, left), netrin-1 and α -Synuclein monomer concentrations were adjusted by BSA assay to begin PFFs reaction with equal amounts of protein (Fig. 4E, right).

Discussion

The current data presented here support a essential and critical role of netrin-1 on the maintenance of mature nigral dopaminergic neurons. Notably, in the adult brain, netrin-1 is mainly expressed in the SNpc of brainstem. Dopaminergic neurons of these brain regions are predominantly impacted by Lewy pathology and neurodegeneration in PD. Targeting PD pathologies underlying the vulnerability of dopaminergic neurons by the specific interactions with α -Synuclein might be one of possible therapeutic approaches to delay or halt neurodegenerative disease progression. However, it is unclear whether the expression pattern of netrin-1 is extensively linked to the selective

maintainability of dopaminergic neuron, and how α -Synuclein modulates the susceptibility of dopaminergic neurodegeneration. Hence, we revealed that depleting endogenous netrin-1 in the primary dopaminergic neuron. Brain-derived neurotrophic factor (BDNF) related to neurodegeneration, induced such a massive cell loss of mature dopaminergic neurons by its depletion (7, 17-19) and presented the similar role of netrin-1 on the maintenance of dopaminergic neurons as shown in the current study. Moreover, we presented the direct interaction between netrin-1 and α -Synuclein via real time binding assay and predictive protein-protein interaction models support the binding affinity between netrin-1 and α -Synuclein at the monomer stage. Considering that Ala 124 ~ Asp 135 regions of α -Synuclein interact with netrin-1, we suppose that netrin-1 can inhibit the hyperphosphorylation of α -Synuclein via various physical interactions. Strikingly, the numbers of PFFs in α -Synuclein + netrin-1 complex were much less than the numbers of PFFs in α -Synuclein only from equal concentration of starting monomer protein materials. These in vitro analyses support that the netrin-1 is the key molecule in α -Synucleinopathies including PD. We also presented that the activation of α -Synuclein expression was associated with the decreased netrin-1 mRNA and protein expression. Taken Together, these findings strongly support that netrin-1 might be a key molecule to develop the therapeutic drug for PD or α -Synucleinopathies.

Materials and Methods

Primary cultured rat dopaminergic neurons, and cell lines

Animal care and handling was performed according to NIH animal care guidelines and Emory Medical School guidelines. Primary rat cortical neurons were cultured as previously described (20). All rats were purchased from the Jackson Laboratory. The protocol was reviewed and approved by the Emory Institutional Animal Care and Use Committee. SH-SY5Y cells were cultured in DMEM/F12 added with 10% FBS and penicillin (100 units/mL)-streptomycin (100 μ g/mL) (all from Hyclone). Cells were incubated at 37 °C in a humidified atmosphere of 5% CO₂. (21)

Cell viability

Cell viability was measured colorimetrically using the Cell-TiterBlue (CTB, Promega, Madison, WI, USA) fluorescence-based assay. Cells were plated at a density of 1000 cells/well in 96-well plates (BD Biosciences, San Diego, CA, USA). Six different PFFs were directly introduced to each well after DIV 10 and then incubated for an additional 4 days. After incubation, 30 μ L CTB reagent was added to each well and incubated at 37 °C and 5% CO₂ for 2.5-5 h. Fluorescence of the resorufin product was measured on a FluoDIA70 fluorescence plate reader (Photon Technology International, Birmingham, NJ, USA). Wells that included vehicle but not protein served as the negative control (0% toxic), and wells containing 10% DMSO were the positive control (100% toxic). Results presented for viability experiments are an average of 3 experiments conducted independently on different days. Error bars represent the standard error of the mean (SEM).

Purification of human α -Syn FL

α -Syn FL cDNAs was subcloned into NdeI and HindIII restriction sites of the bacterial expression vector pRK172, and the proteins were expressed in Escherichia coli BL21 (DE3). Bacterial pellets were resuspended in high-salt buffer (0.75 M NaCl, 50 mM Tris, pH 7.4, 1 mM EDTA) containing a mixture of fresh protease inhibitors, sonicated at 25% power for 3 min in the ice (3 times), and centrifuged at 70,000 \times g for 30 min. We used thrombin to remove His tag. After that, α -Syn FL proteins were dialyzed in FPLC buffer (50 mM NaCl, 50 mM Tris-HCl, pH 7.4) overnight at 8 °C to change the buffer salt concentration. Proteins were filtered through a 0.22 μ m syringe filter and injected into the FPLC machine (Superdex 200 column; GE Healthcare). The fractions were assayed for the presence of the α -Syn FL protein by SDS-PAGE followed by Coomassie Blue staining. (22)

Generation of α -Syn FL PFFs

Fibrils were prepared in reaction (500 μ L per tube) containing 5 mg/mL of α -Syn FL and α -Syn FL (5 mg/mL) + NTN1 (5 mg/mL) protein monomers in PFF reaction buffer (50 mM Tris-HCl, 50 mM NaCl, pH 7.4). The monomer proteins were incubated for several days at 37 °C, with orbital shaking at 300 rpm until samples appeared cloudy. Usually, the reactions were subjected to 8-10 days shaking for the PFFs generation. PFFs were validated by Th-T in

vitro assay.

Th-T assay

Thioflavin T stock solution was made by dissolving 16 mg Th-T to 50 mL PBS. Solution was filtered through a 0.2 μ m syringe filter (Sigma-Aldrich, cat# T3516). The stock solution was diluted into the PBS to inject the working concentration (2.5 μ L of 1 mM Th-T stock solution per each well of 96-well plate). The monomers and PFFs were added according to the working concentration (10 μ M). The total volume per each well was fixed to 100 μ L. The rest volume except for Th-T solutions and proteins was filled with phosphate buffer. Reaction plate was excited at 450 nm and emitted at 490 nm to measure the relative fluorescence units on the plate reader (Molecular Devices, SpectraMax iD3, California, USA). Measurements were conducted every 15 minutes.

Biacore X100 (Real Time Binding Assay)

The carboxylated dextran matrix of the sensor chip was activated by the injection of 60 μ L of solution containing 0.2 M N-ethyl-N'-(3-dimethylaminopropyl) carbodiimide and 0.05 M N-hydroxysuccinimide in water. We used the activation buffers from the kit, EDC + NHS. Immobilization step running time was 180s. Purified α -Syn FL proteins were immobilized at a concentration of 50 μ g/mL in 10 mM sodium acetate (pH 4.0). 50 mM NaOH was employed for regeneration in 75 μ L, maximum volume of deionized water and running buffer (HEPES + EDTA + P20) (BIAcore, GE Healthcare). The remaining binding sites were blocked with 1M ethanolamine (pH 8.5). Screening of purified netrin-1 proteins for binding to α -Syn FL was performed by injecting aliquots (120 μ L) of samples (~100 μ g protein/mL) onto the derivatized sensor chip. CM5 chip was used for regeneration step. Regeneration of sensor chip after each analysis cycle was performed by injecting 20 μ L of 1.5 M glycine/HCl buffer (pH 3.5) and 6 M guanidinium HCl (pH 5.5).

Transmission electron microscopy (TEM)

Electron microscopy images were produced from α -Syn FL and α -Syn FL + NTN1 after PFFs were generated. The samples (5 μ L) were deposited on Formvar-coated 400 mesh copper grids, fixed with 0.5% glutaraldehyde, negative

stained with 2% uranyl acetate (Sigma-Aldrich, Germany) and screened by CM-10 TEM.

X-ray diffraction (XRD)

Dried stock samples were prepared for X-ray fiber diffraction by vortexing α -Syn FL and α -Syn FL + NTN1 PFFs for 30 min at RT. The PFFs were lyophilized for 3 days using a freeze-drying machine for X-ray diffraction. The sample-to-detector distance was 300 mm, with an exposure time of 30 sec. Diffraction patterns were converted to Tiff files using the program fit-2d (Hammersley/ESRF) and radially integrated to generate one-dimensional scattering patterns using Matlab code. The position of maximum intensity was used to determine the position of anionic reflections and the difference in position of either side of the pattern was used to assess the error in the position of the reflection. The variation in X-ray intensity for the reflections at α -Syn FL PFFs 4.49 Å and 4.05 Å ; α -Syn FL + NTN1 PFFs 4.49 Å and 4.06 Å (fibril reaction buffer: 50 mM Tris-HCl, 50 mM NaCl, pH 7.0). Moreover, we determined X-ray intensity using the same Matlab code. A calibrant of high density polyethylene (HDPE) was used to determine the position of the beam sample-to-detector distance and pixel size.

Immunofluorescence

Free-floating slices were rinsed in PBS then permeabilized and blocked with PBS-BT (50 mM Tris-HCL, 150 mM NaCl, 3% bovine serum albumin (BSA), 0.1% Triton-X100, pH 7.4) blocking solution for 1 h. Afterwards, the sections were incubated with primary antibodies (see key resource table) in a 2% normal donkey serum (NDS) and 0.3% Triton X-100 PBS solution on a shaker overnight at 4 °C. The next day, sections were rinsed and incubated with corresponding secondary antibodies directly conjugated with fluorophores (1:2000 Alexa 594 and Alexa Fluor 488 conjugate from Jackson ImmunoResearch) for 2 h at room temperature. Finally, slices were rinsed in PBS and mounted (Sigma Aldrich, F4680).

Immunoblotting

Cells and brain samples were lysed and, if necessary, homogenized in lysis buffer (50 mM Tris, pH 7.4, 40 mM NaCl, 1 mM EDTA, 0.5% Triton X-100, 1.5 mM Na₃VO₄, 50 mM NaF, 10 mM sodium pyrophosphate and 10 mM sodium β -glycerophosphate, supplemented with a cocktail of protease inhibitors). Lysates were then centrifuged for 20 min at 4 °C 15000 rpm and protein concentration of the supernatant was measured with the Pierce BCA Protein Assay Kit (Part No. 23225). The supernatant was denatured at 95 °C in Laemmli buffer. After loading and running proteins in a SDS-PAGE gel, the samples were transferred to a nitrocellulose membrane. Membrane blocking and antibody staining were performed according to the primary antibody manufacturer's instructions. Primary antibodies to the following targets were used: alpha synuclein FL (Santa Cruz, Cat# SC69977) alpha-synuclein pS129 (LS bio, Cat# LS-C380861-1); Tyrosine Hydroxylase (Santa Cruz, SC-25269; Abcam, Cat# ab112); Netrin-1 (Santa Cruz, Cat# SC20786 or SC-293197; Abcam, Cat# ab126729); Netrin-3 (Abcam, Cat# ab185200); Netrin-4 (Santa Cruz, Cat# SC365280) MAO-B (Abcam, Cat# ab133270) and cleaved caspase-3 (Cell signaling Cat# 9661).

TUNEL assay

Dopamine neuron death was detected with an *in-situ* cell death detection kit TMR Red (Roche, Cat# 12156792910). The apoptotic index was expressed as the percentage of TUNEL positive neurons out of the total number of TH-positive neurons.

Mouse midbrain primary neuron culture

Dopamine primary neurons were prepared from the ventral midbrain of embryonic mice on day 13 of gestation. Ventral midbrain was isolated and dissected in ice-cold Dulbecco's medium + 0.2% BSA. Fragments were dissected into tiny pieces and collected in 2 mL vials. Then, pieces were washed three times in HBSS (Ca²⁺ and Mg²⁺ free) medium. Pieces were dissociated in HBSS containing 0.01% trypsin for 20 min at 37 °C. Cells were dissociated by soft trituration in FBS medium containing 1 μ g/mL of DNase I. After trituration, cells were washed in DA neuron culture medium (DMEM F12, N2 1X, 0.36% D-(+)-Glucose (wt/vol), primocin 100 μ g/mL) and plated on 96-well plates coated with poly-L-ornithine at a density of 5×10^4 cells/well and let to adhere for 1 hour. Then, cells were treated

with netrin-1 or GDNF. The treatment was renewed every two days for four days.

Netrin-1 Gene-Expression Profiling Dataset

Netrin-1, -3 and -4 gene expression profiling in the SN of PD patients was conducted using a gene dataset available on the GEO repository (GDS2821 accession number). We selected this dataset because the corresponding study (23) included a large number of participants, 9 control patients and 16 PD patients, and very strict RNA quality control criteria were used. Gene expression profiling was done using Affymetrix Human Genome U133 Plus 2.0 GeneChip arrays. We analyzed probe set data for NTN1, NTN3, and NTN4 in the substantia nigra and selected NTN1 probe set on the criterion of “present” (detectable) call. GeneMANIA software was used to investigate actual molecular interactions and common pathway among netrin family and α -Synuclein. Data were collected from primary studies found in various databases, including BioGRID, PathwayCommons, Reactome and BioCyc (24, 25).

Protein-protein interaction prediction analysis

Protein-protein interaction was analyzed and visualized by ClusPro 2.0 (<https://cluspro.bu.edu/>) and PyMOL 2.5 (<https://pymol.org/2/>) software. Protein Data were collected Protein Data Bank (PDB, USA) and PDB files for netrin-1 and α -Synuclein were entered into receptor protein and ligand protein. Binding residues are presented as the technical preset mode and modified with an extensive binding atomic groups per one residue. Polar contacts, inter-chain contacts, and pi interactions were investigated at the target amino acid regions (26, 27)

Quantification and statistical analysis

All data are expressed as mean \pm S.E.M. from three or more independent experiments. Representative morphological images obtained from at least 3 experiments with similar results were provided. Image J 1.47 software was used to analyze IF experiments, and Image Lab™ software for western blots analysis. The statistical analysis of results was performed using GraphPad5 (Prism) software. All data were tested for normal distribution in order to analyze results accordingly using parametric or non-parametric tests. To compare results between two groups, the Student's unpaired t-test was used. When more than two groups were compared, one-way ANOVA followed by Tukey post hoc test was

applied. For repeated measures, a Repeated-Measures (RM) ANOVA or 2way ANOVA test was performed followed by Tukey multiple comparisons post hoc test. Assessments with $p < 0.05$ were considered significant.

Acknowledgements

We thank Seong Su Kang (Department of Pathology and Laboratory Medicine, Emory University) Emory University for their excellent experiment technical assistance.

Conflict of interest

The authors declare that they have no competing interests.

Figure Legends

Fig 1. Investigation of gene expression level among Netrin-1, -3, and -4 from PD patients and non-PD (healthy control)

(A) Netrin-1 (left), -3, (middle), and -4 (right) gene expression profiling by mRNA of SN from PD and healthy controls through GEO database profiling, accessed with GDS2821. Unpaired t-test, $**P < 0.01$; N.S., not significant.

(B-D) Human protein interaction map from (<http://www.genemania.org>). Each network was visualized with red line (physical interactions).

(E) Netrin-1, -3, and -4 gene expression data from 3 healthy adults brains. Microarray data were come from Allen Human Brain Atlas. Codes at the right of the heatmap are probes used in the analysis. MRI images including expression level at SNc part, detected with the same probe, are below the microarray data.

Fig 2. Direct interaction between netrin-1 and α -Synuclein

(A) Real time binding assay with SPR Biacore X100 using the CM5 chip as a binding ligand. In vitro test was conducted with purified hnetrin-1 and h α -synuclein recombinant proteins.

(B-D) Predictive three-dimensional model of direct interaction structures between netrin-1 (PDB ID: AF-O95631-F1) and α -Synuclein (PDB ID: AF-P37840-F1) by ClusPro 2.0 and PyMOL 2.5 software analysis. Balanced model, electrostatic-favored model, and van der Waals force-favored model showed the polar contacts between netrin-1 and α -Synuclein.

Fig 3. Dopaminergic neuronal loss accompanied by the deprivation of netrin-1

(A) Co-immunofluorescence staining analysis upon DCC-4Fbn or control IgG treatment primary dopaminergic neurons conducted by TH/MAP2, MAP2/NTN1, and MAP2/pS129 (Scale bar, 50 μ m).

(B) Quantification bar graph of TH, MAP2, NTN1, and pS129 immunoreactive positive dopaminergic neuron cell numbers. Data are shown as mean + SEM. Statistical significance was determined by an unpaired t-test. N= 4 each group. $**P < 0.01$.

(C) Terminal deoxynucleotidyl transferase (TdT) dUTP Nick-End Labelling (TUNEL) reactivity in primary dopaminergic neurons after control IgG and DCC-4Fbn treatments (Scale bar, 40 μ m).

(D) DNA fragmentation index (bar graph) expressed as a percentage of TUNEL positive dopamine (DA) neurons out of the total number of MAP2-positive neurons. N = 3 each group. Error bars represent the mean \pm SEM. Statistical significance was conducted using a one-way ANOVA followed by post hoc Tukey test for multiple group comparison. $**P < 0.01$.

(E) Immunoblotting assay of netrin-1, TH, MAO-B, cleaved caspase-3, α -Syn pS129 and β -actin levels in control IgG (N=3) vs DCC-4Fbn treated cell lysates (N=3). Band intensity quantification bar graph (right).

(F) Immunoblot of SH-SY5Y cell lysates with treated neurotoxin MPP⁺ in a dose-dependent manner (1-3 mM). Relative band intensity were calculated from the band densitometry software (Image J). Quantification of band intensity (right). N=3 independent immunoblot assay. Error bars represent the mean \pm SEM. Statistical significance was determined by Student's t-test. $*P < 0.05$; $**P < 0.01$; N.S., not significant.

Fig 4. Structural analyzes for pre-formed fibrils (PFFs) with verification netrin-1 as an inhibitor of α -Synuclein fibrilization

(A) Thioflavin T assay showed that different aggregation rates of purified h α -Syn, h α -Syn + hNTN1 combination at different day of PFFs generation reactions.

(B) h α -Syn + hNTN1 complex aggregate and form fibrils much less than h α -Syn only group on reaction day 10. Results are shown as means \pm SEM; N=3 independent experiments; ** P < 0.01 by two-tailed Student's t-test.

(C) X-Ray diffraction pattern of partially aligned h α -Syn

(D) X-Ray diffraction pattern of partially aligned h α -Syn + hNTN1.

(E) Negative stained TEM images of h α -Syn and h α -Syn + hNTN1 complex on day 10 (left). Coomassie blue staining results supported that each PFFs were generated under equal concentrations and ratios (right).

References

1. Serafini T, Kennedy TE, Galko MJ, Mirzayan C, Jessell TM and Tessier-Lavigne M (1994) The netrins define a family of axon outgrowth-promoting proteins homologous to *C. elegans* UNC-6. *Cell* 78, 409-424
2. Serafini T, Colamarino SA, Leonardo ED et al (1996) Netrin-1 is required for commissural axon guidance in the developing vertebrate nervous system. *Cell* 87, 1001-1014
3. Lauderdale JD, Davis NM and Kuwada JY (1997) Axon tracts correlate with netrin-1a expression in the zebrafish embryo. *Mol Cell Neurosci* 9, 293-313
4. Tang X, Jang SW, Okada M et al (2008) Netrin-1 mediates neuronal survival through PIKE-L interaction with the dependence receptor UNC5B. *Nat Cell Biol* 10, 698-706
5. Rajasekharan S and Kennedy TE (2009) The netrin protein family. *Genome Biol* 10, 239
6. Yamagishi S, Yamada K, Sawada M et al (2015) Netrin-5 is highly expressed in neurogenic regions of the adult brain. *Front Cell Neurosci* 9, 146
7. Ahn EH, Kang SS, Liu X et al (2021) BDNF and Netrin-1 repression by C/EBP β in the gut triggers Parkinson's disease pathologies, associated with constipation and motor dysfunctions. *Prog Neurobiol* 198, 101905
8. Jasmin M, Ahn EH, Voutilainen MH et al (2021) Netrin-1 and its receptor DCC modulate survival

- and death of dopamine neurons and Parkinson's disease features. *EMBO J* 40, e105537
9. Blesa J and Przedborski S (2014) Parkinson's disease: animal models and dopaminergic cell vulnerability. *Front Neuroanat* 8, 155
 10. Olanow CW and Brundin P (2013) Parkinson's disease and alpha synuclein: is Parkinson's disease a prion-like disorder? *Mov Disord* 28, 31-40
 11. Armstrong MJ and Okun MS (2020) Diagnosis and Treatment of Parkinson Disease: A Review. *JAMA* 323, 548-560
 12. Kang SS, Ahn EH, Zhang Z et al (2018) alpha-Synuclein stimulation of monoamine oxidase-B and legumain protease mediates the pathology of Parkinson's disease. *EMBO J* 37
 13. Li W, Lesuisse C, Xu Y, Troncoso JC, Price DL and Lee MK (2004) Stabilization of alpha-synuclein protein with aging and familial parkinson's disease-linked A53T mutation. *J Neurosci* 24, 7400-7409
 14. Yoo H, Lee J, Kim B et al (2022) Role of post-translational modifications on the alpha-synuclein aggregation-related pathogenesis of Parkinson's disease. *BMB Rep* 55, 323-335
 15. Anderson JP, Walker DE, Goldstein JM et al (2006) Phosphorylation of Ser-129 is the dominant pathological modification of alpha-synuclein in familial and sporadic Lewy body disease. *J Biol Chem* 281, 29739-29752
 16. Paradisi A, Maisse C, Coissieux M-M et al (2009) Netrin-1 up-regulation in inflammatory bowel diseases is required for colorectal cancer progression. *Proceedings of the National Academy of Sciences* 106, 17146-17151
 17. Bathina S and Das UN (2015) Brain-derived neurotrophic factor and its clinical implications. *Arch Med Sci* 11, 1164-1178
 18. Howells DW, Porritt MJ, Wong JY et al (2000) Reduced BDNF mRNA expression in the Parkinson's disease substantia nigra. *Exp Neurol* 166, 127-135
 19. Loeliger MM, Briscoe T and Rees SM (2008) BDNF increases survival of retinal dopaminergic neurons after prenatal compromise. *Invest Ophthalmol Vis Sci* 49, 1282-1289
 20. Zhang Z, Song M, Liu X et al (2014) Cleavage of tau by asparagine endopeptidase mediates the neurofibrillary pathology in Alzheimer's disease. *Nat Med* 20, 1254-1262
 21. Zhang Z, Kang SS, Liu X et al (2017) Asparagine endopeptidase cleaves α -synuclein and mediates pathologic activities in Parkinson's disease. *Nature structural & molecular biology* 24, 632-642
 22. Ahn EH, Kang SS, Liu X et al (2020) Initiation of Parkinson's disease from gut to brain by δ -secretase. *Cell Research* 30, 70-87
 23. Papapetropoulos S and Singer C (2006) Psychiatric comorbidity in a population of Parkinson's disease patients. *Eur J Neurol* 13, e1
 24. Wang X, Cimerancic P, Yu C et al (2017) Molecular Details Underlying Dynamic Structures and

- Regulation of the Human 26S Proteasome. *Mol Cell Proteomics* 16, 840-854
25. McFarland MA, Ellis CE, Markey SP and Nussbaum RL (2008) Proteomics analysis identifies phosphorylation-dependent alpha-synuclein protein interactions. *Mol Cell Proteomics* 7, 2123-2137
 26. Kozakov D, Hall DR, Xia B et al (2017) The ClusPro web server for protein-protein docking. *Nat Protoc* 12, 255-278
 27. Desta IT, Porter KA, Xia B, Kozakov D and Vajda S (2020) Performance and Its Limits in Rigid Body Protein-Protein Docking. *Structure* 28, 1071-1081 e1073

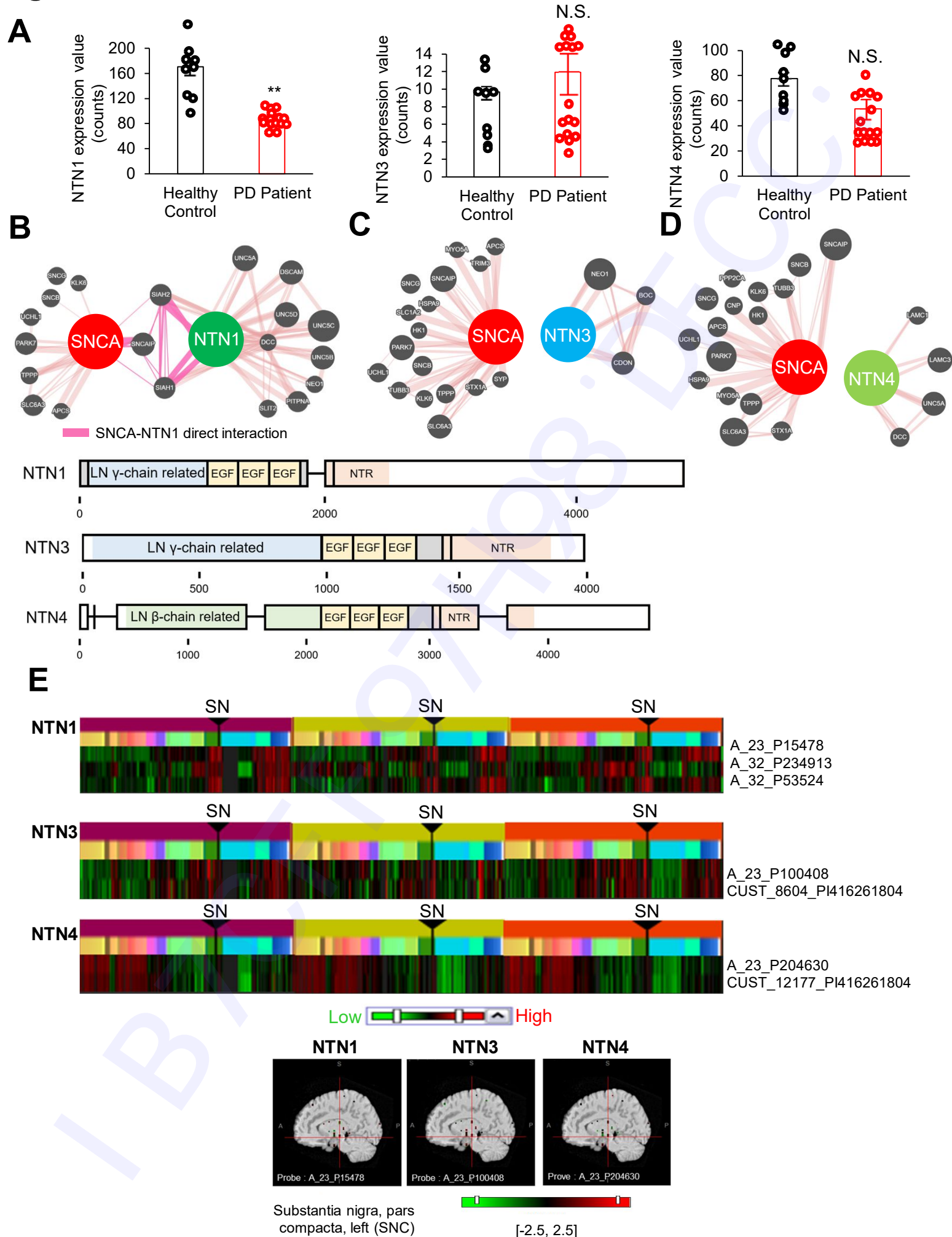
Fig. 1

Fig. 2

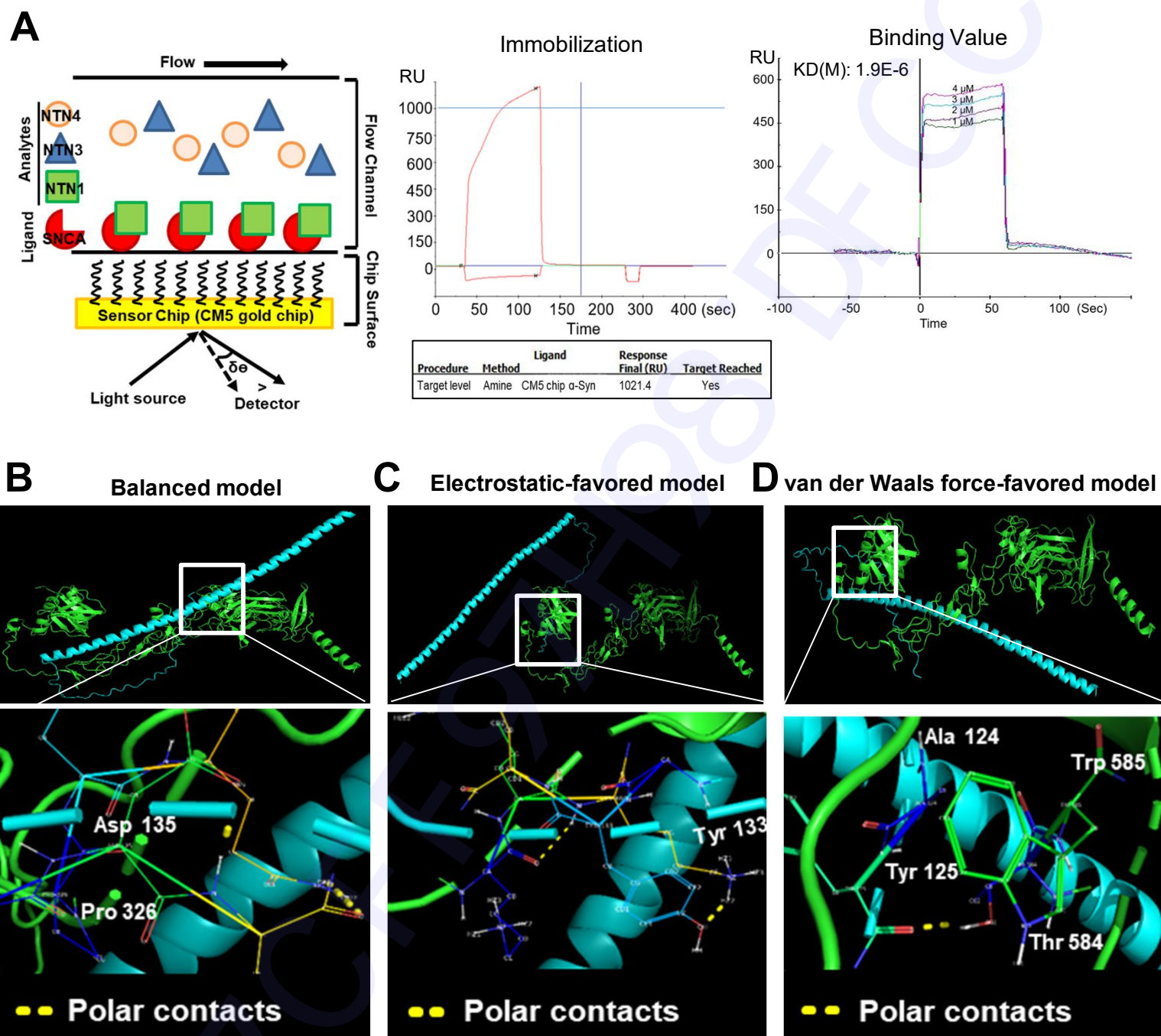


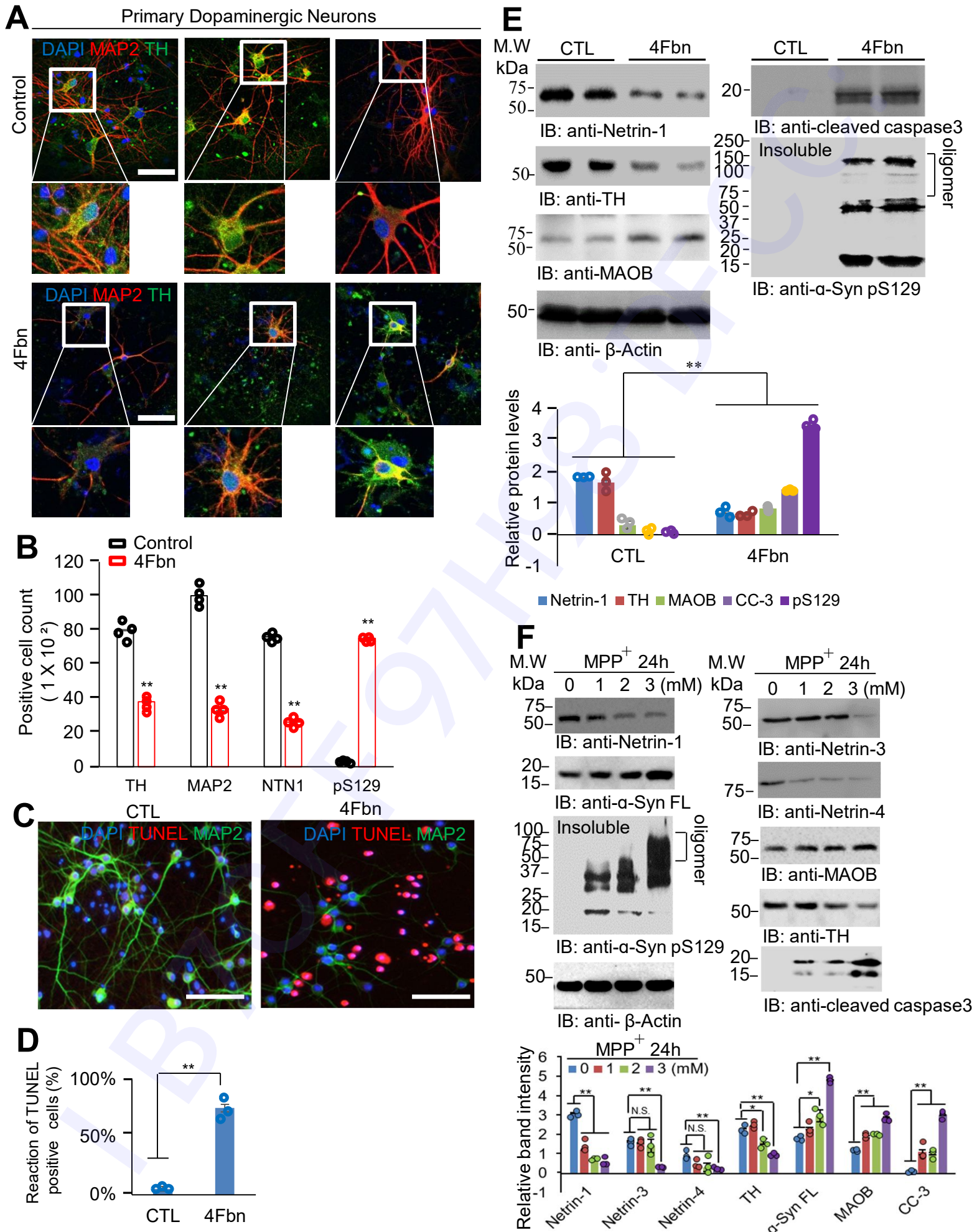
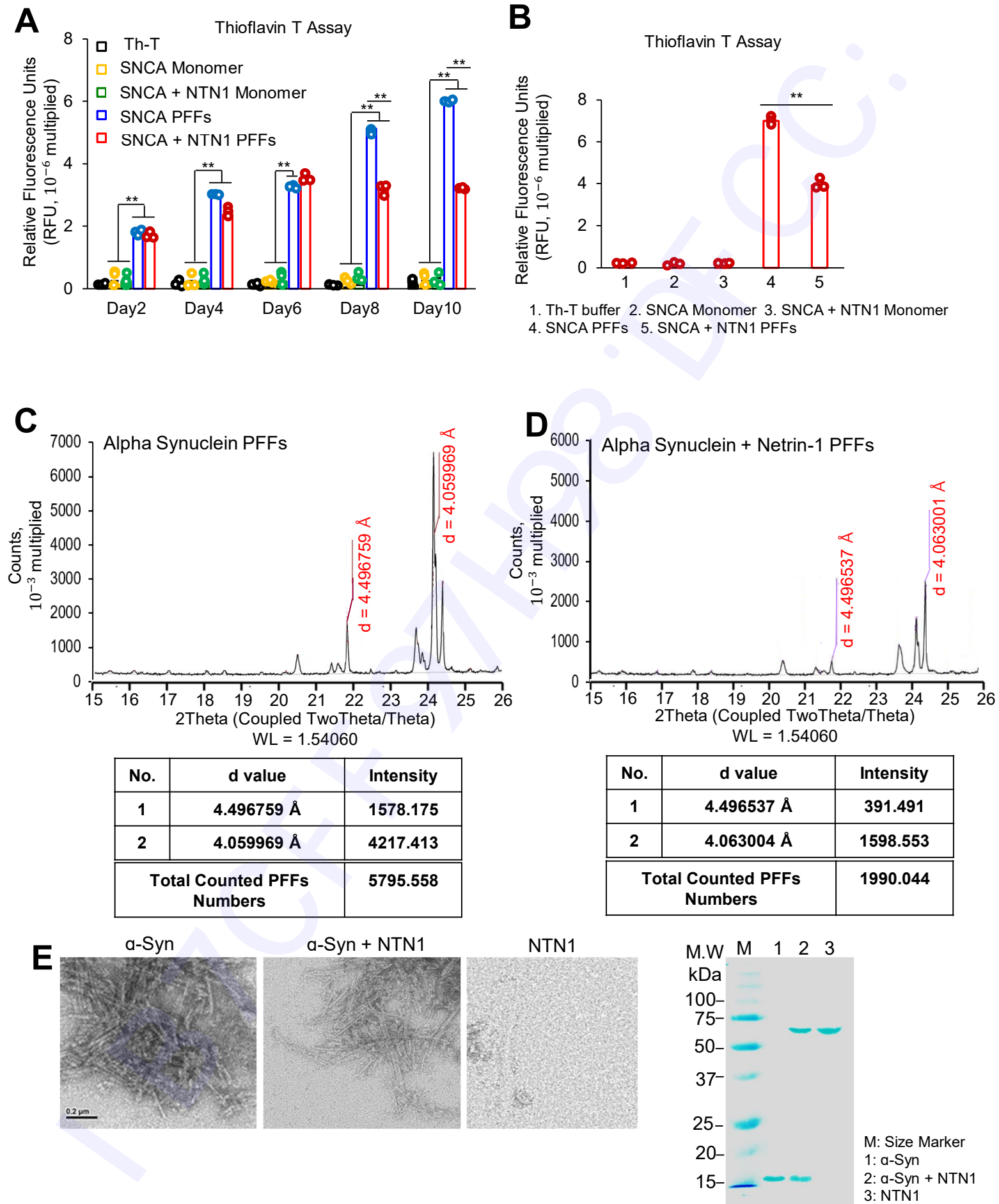
Fig. 3

Fig. 4

The couple of netrin-1/ α -Synuclein regulates the survival of dopaminergic neurons via α -Synuclein disaggregation

Eun Ji Kang¹, Seung Min Jang¹, Ye Ji Lee¹, Ye Ji Jeong¹, You Jin Kim¹, Seong Su Kang², and Eun Hee Ahn^{1*}

¹Department of Physiology, College of Medicine, Hallym University, Hallymdaehak-gil 1, Chuncheon-si, Gangwon-Do 24252, South Korea

²Department of Pathology and Laboratory Medicine, Emory University School of Medicine, Atlanta, GA 30322, USA

Address for correspondence

Prof. Eun Hee Ahn

Department of Physiology, College of Medicine, Hallym University, Hallymdaehak-gil, Chuncheon-si, Gangwon-Do 24252, South Korea

Email : eunhee.ahn@hallym.ac.kr

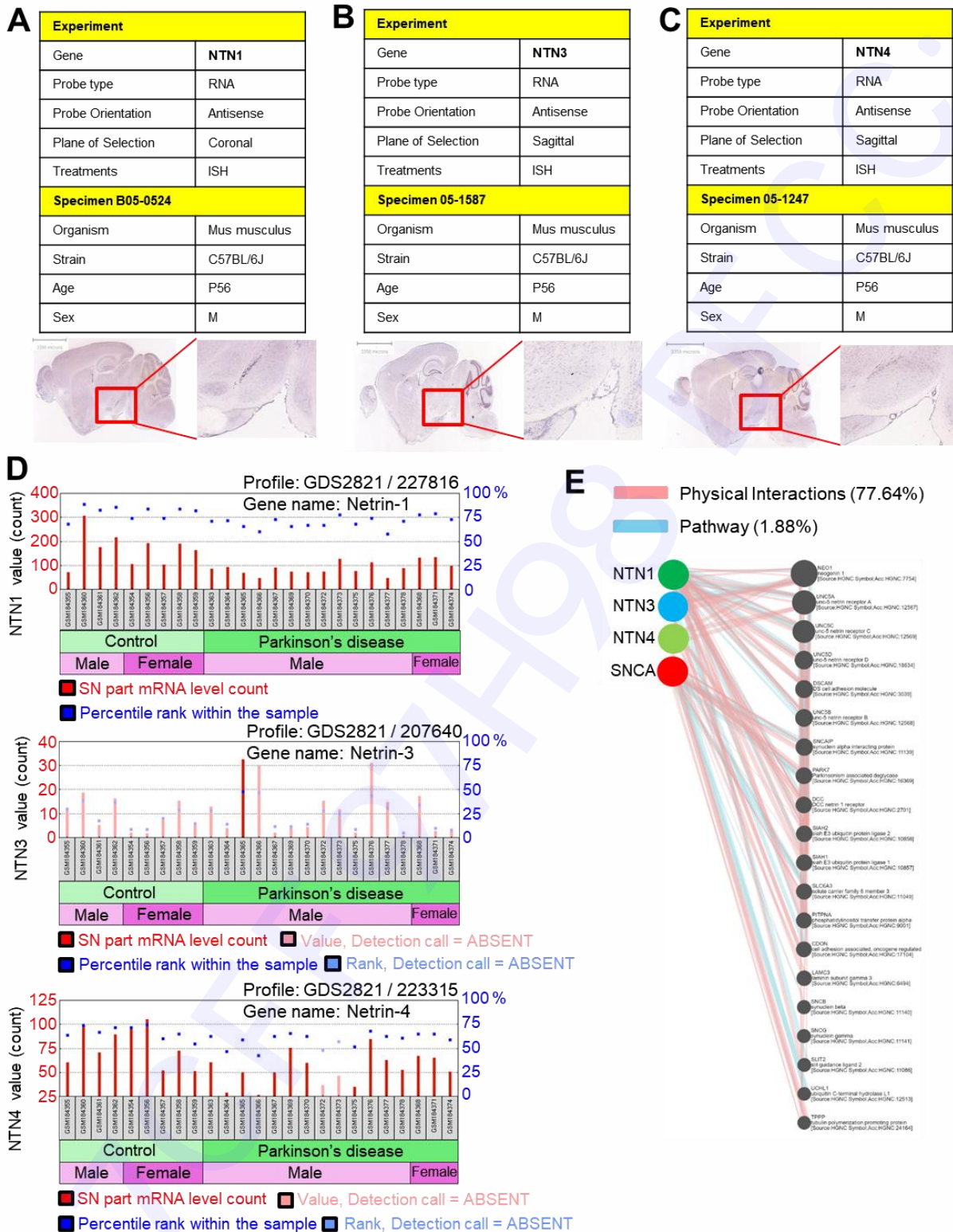
Supplemental information

Supplementary Fig. 1 shows the correspondence of netrin family expression levels between human and mouse through Allen human brain atlas data and GEO database analysis. Netrin-1 is highly expressed in the SN region both human and mouse mRNA levels. It also shows the physical interactions and shared pathways between α -Synuclein and netrin family.

Supplementary Fig. 2 shows that netrin-1 can reduce hyperphosphorylation of α -Synuclein S129 in dopamine neurons. It also shows the re-reducing neurotoxicity via netrin-1 treatment in the SNCA overexpressed dopaminergic neurons.

Supplementary Fig. 3 shows the correlation between dopaminergic neuronal cell survival and netrin-1 deprivation through DCC-4Fbn treatment. DCC-4Fbn induce escalation of pS129 level, which is hyperphosphorylated state of α -Synuclein. It also shows that AAV-SNCA virus infected dopaminergic neuron have similar tendency described before.

Supplementary Fig. 4 shows neurotoxin or netrin-1 reductive factors induce intracellular ROS and DNA fragmentation, triggering cell deaths.



Supplementary Figure 1. Netrin-1 is deprived clearly in PD patient's SN part, showing the strongest molecular interactions with SNCA

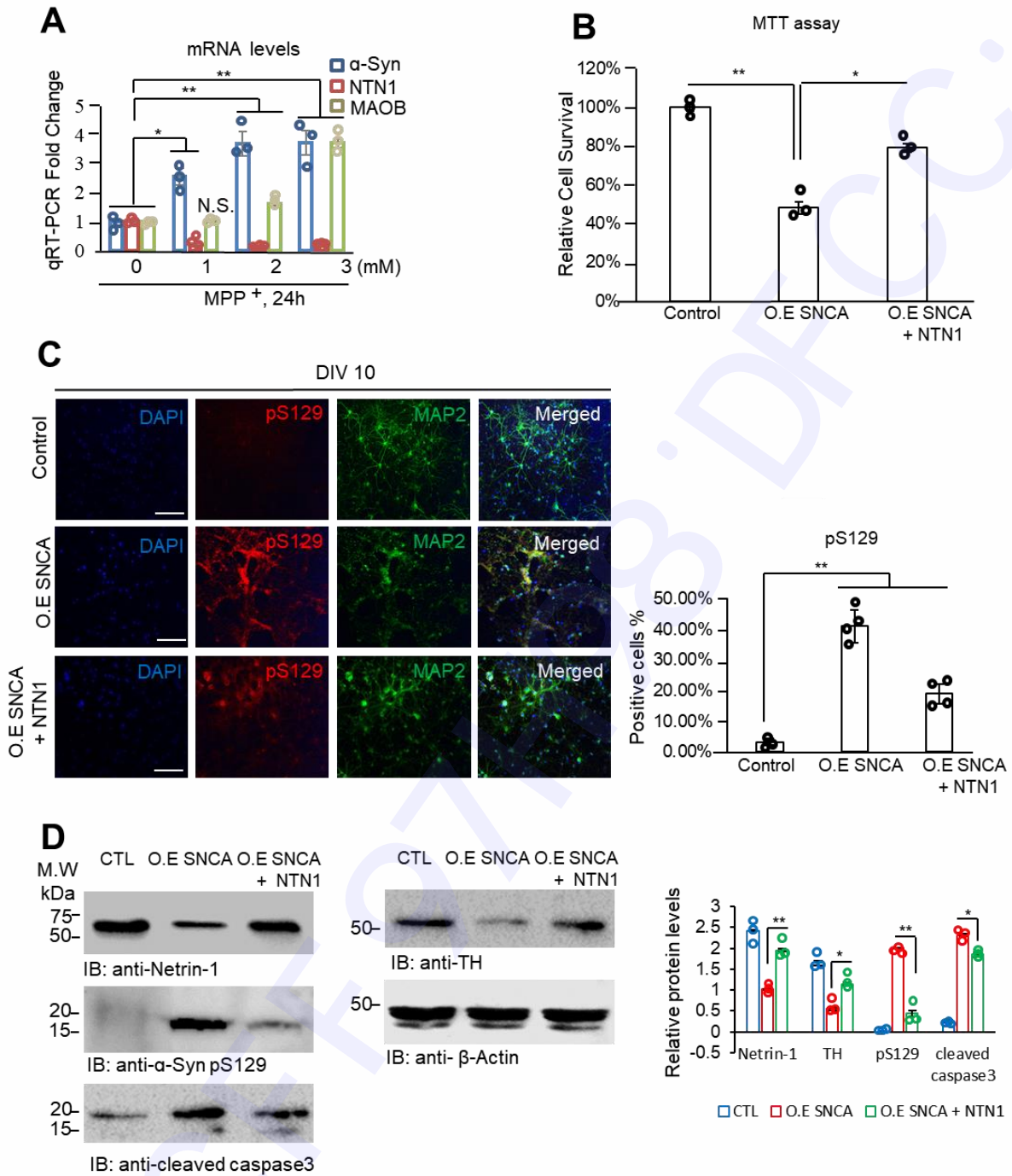
(A) In situ hybridization (ISH) images and visualized netrin-1 expressed regions in midbrain of C57BL/6J.

(B) ISH images and visualized netrin-3 expressed regions.

(C) ISH images and visualized netrin-4 expressed regions. Selected direction is Sagittal, and scale bars were shown identically as 3356 microns.

(D) Netrin-1, -3, and -4 expression profiling in SN part. GDS2821 is the code for accession, and each values were collected from 9 healthy controls and 16 PD patients.

(E) Netrins/SNCA Physical interactions (Red line, 77.64%) and shared molecular signal pathways (Blue line, 1.88%).



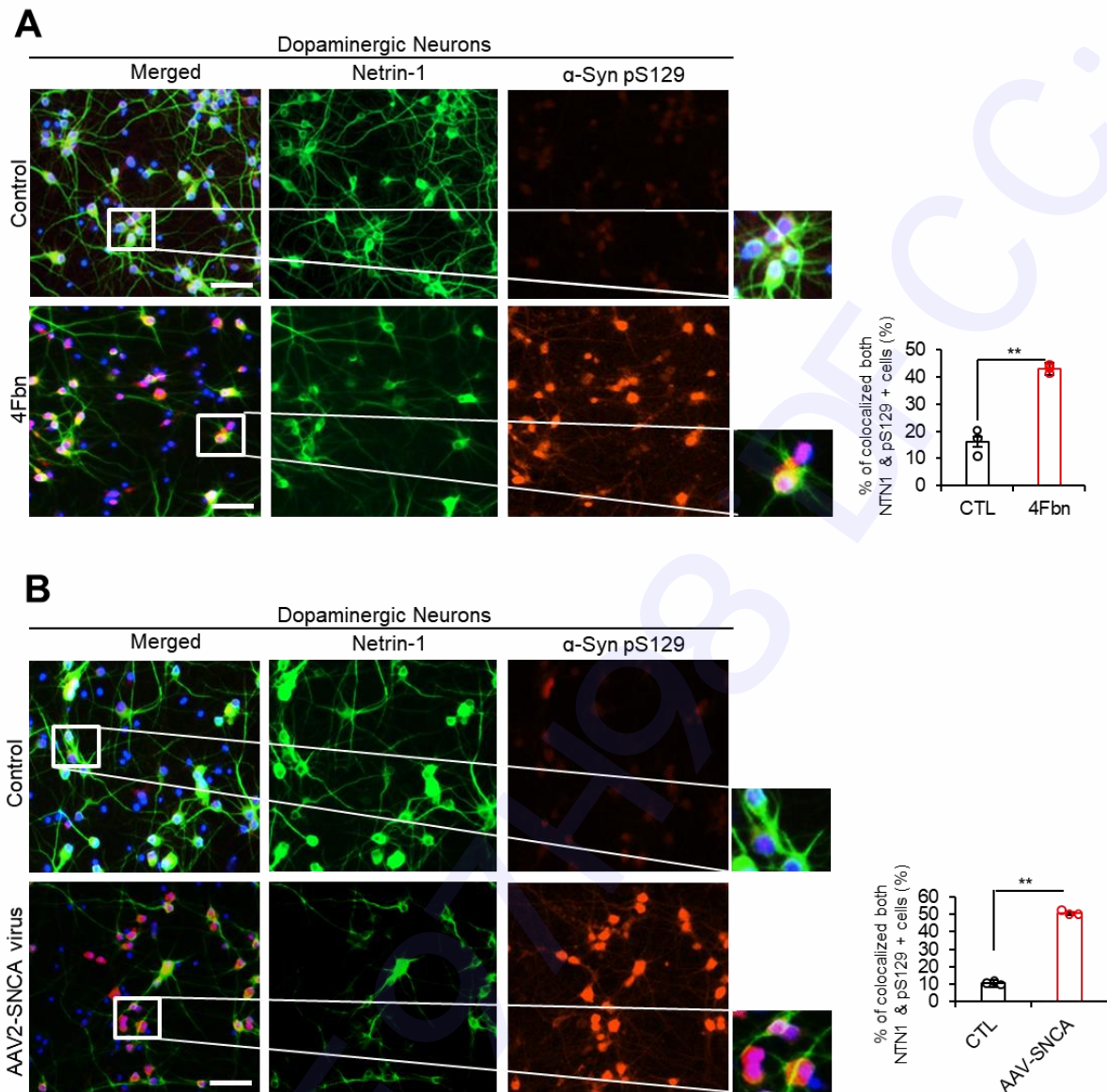
Supplementary Figure 2. Comparison of cellular and neuronal viability between overexpressed SNCA group vs overexpressed SNCA + hNTN1

(A) qRT-PCR fold changes and mRNA levels of α -Syn, NTN1, and MAOB under the MPP⁺ treated for 24 h, dose-dependently (0, 1, 2, 3 mM).

(B) Cell survival counts were calculated through MTT assay, netrin-1 elevated relative cell survival values than overexpressed SNCA only.

(C) Co-immunofluorescence staining of α -Syn pS129 (red) /MAP2 (green). Scale bar, 20 μ m.

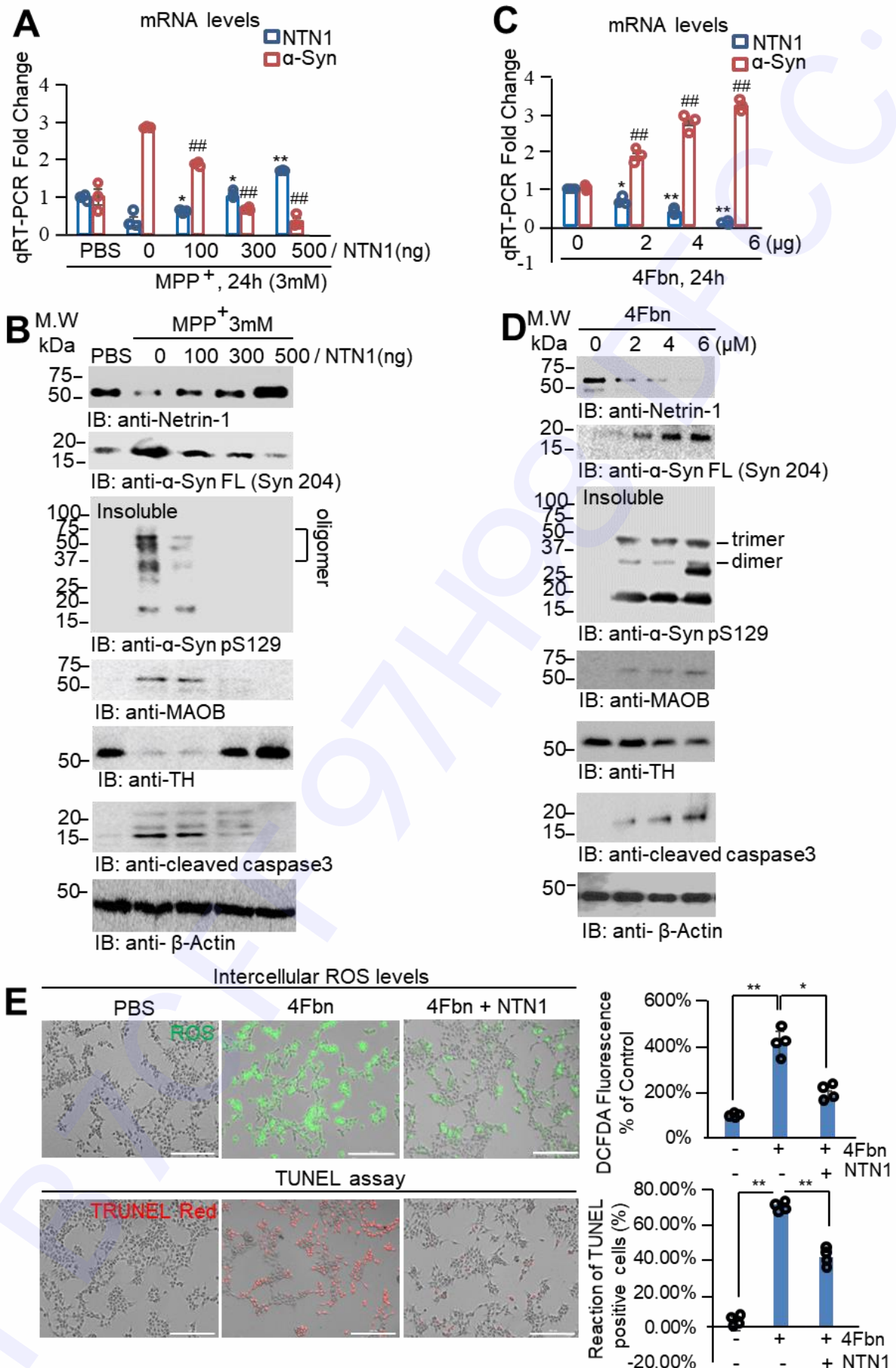
(D) Immunoblot on CTL, overexpressed-SNCA, and overexpressed-SNCA + hNTN1 200 ng treated DIV 10 lysates showing the modulation of netrin-1, α -Syn pS129, cleaved caspase-3, and TH levels. N=3 each group. Unpaired t-test * $P < 0.05$; ** $P < 0.01$.



Supplementary Figure 3. Netrin-1 depletion in dopaminergic neurons increases α -Syn pS129 formation

(A) Co-immunofluorescence staining with Netrin-1 and pS129 validated that netrin-1 deprivation in 4Fbn-treated neuron contributed to the neuronal death.

(B) In AAV6-SNCA virus injected neurons, toxic α -Synuclein (α -Syn pS129) levels were highly increased compared to the control group.



Supplementary Figure 4. Neurorestorative effect measurements of netrin-1 in dopamine cell model

(A) SH-SY5Y cells were treated with 0-500 ng of recombinant netrin-1 protein under neurotoxin stress for 24 h. Netrin-1 and α -Syn mRNA levels conducted by qRT-PCR. N=3 independently experiments. Error bars represent the mean \pm SEM. Statistical significance was conducted using a one-way ANOVA followed by post hoc Tukey test for multiple group comparison. $*P < 0.05$; $**P < 0.01$ (NTN1); $###P < 0.01$ (α -Syn).

(B) Immunoblot showed the netrin-1, α -Syn FL, insoluble α -Syn pS129, MAOB, TH, cleaved caspase-3, and β -actin levels.

(C) DCC-4Fbn dose-dependently (0-6 μ g) reduced netrin-1 mRNA level. N=3 independently experiments. Error bars represent the mean \pm SEM. Statistical significance was conducted using a one-way ANOVA followed by post hoc Tukey test for multiple group comparison. $*P < 0.05$; $**P < 0.01$ (NTN1); $###P < 0.01$ (α -Syn).

(D) Immunoblot results identical with (B), PD marker protein (α -Syn FL, insoluble α -Syn pS129, MAOB, TH, and cleaved caspase-3).

(E) Representative images for DCF-DA (intracellular ROS) dye positive cell intensity in DCC-4Fbn vs DCC-4Fbn + NTN1 protein treated group (upper). DCF-DA fluorescence intensity quantification bar graph on the upper right panel. TUNEL assay representative images (bottom left) and quantification bar graph (bottom right) showed the recombinant netrin-1 protein neurorestorative effect. N=4 independently experiments (Scale bar, 20 μ m). Error bars represent the mean \pm SEM. Statistical significance was conducted using a one-way ANOVA followed by post hoc Tukey test for multiple group comparison. $*P < 0.05$; $**P < 0.01$.

Supplementary Table 1. Abbreviations

Abbreviations

AAV: Adeno-associated Virus

BDNF: Brain-derived Neurotrophic Factor

DA: Dopaminergic

DCC-4Fbn: 4th fibronectin domain of Deleted in Colorectal Cancer

FL: Full Length

GDNF: Glial cell-derived Neurotrophic Factor

GEO: Gene Expression Omnibus

GST: Glutathione S-Transferase

HDPE: High Density Polyethylene

hNTN1: human NTN1

HPC: Hippocampus

IF: Immunofluorescence

KO: Knock-out

LAL: Limulus Amebocyte Lysate

MAO-B: Monoamine Oxidase B

MAP2: Microtubule-associated Protein 2

MPP⁺: 1-methyl-4-phenylpyridinium

NTN1: Netrin-1

NTN3: Netrin-3

NTN4: Netrin-4

PD: Parkinson's Disease

PFFs: Pre-formed fibrils

pS129: Phosphorylated α -Synuclein at the residue S129

qRT-PCR: Quantitative RT-PCR

SN: Substantia Nigra

SNpc or SNc: Substantia Nigra pars compacta

Tg: Transgenic

TH: Tyrosine Hydroxylase

Th-T: Thioflavin-T

VTA: Ventral Tegmental Area

WT: Wild-type

α -Syn: α -Synuclein